phys. stat. sol. (a) **173**, 93 (1999)

Subject classification: 68.45.Da; S10.1

Thermodesorption of CO and NO from Vacuum-Cleaved NiO(100) and MgO(100)

R. WICHTENDAHL, M. RODRIGUEZ-RODRIGO, U. HÄRTEL, H. KUHLENBECK[1]), and H.-J. FREUND

Fritz-Haber-Institut der Max-Planck-Gesellschaft, Abteilung Chemische Physik, Faradayweg 4–6, D-14195 Berlin, Germany

(Received September 20, 1998)

This paper presents experimental data on the bonding of CO and NO to vacuum-cleaved MgO(100) and NiO(100) and compares them with theoretical results. In the case of CO and NO on NiO(100) we find that the bonding energies obtained for the vacuum-cleaved single crystals agree well with results of recent studies on thin NiO(100) films grown by oxidation of Ni(100) whereas they are at variance with theoretical results. On the other hand, for CO on MgO(100) the experimental data fit well to recent theoretical studies while they contradict studies of adsorption on MgO(100) films grown on Mo(100). The experimentally determined values for the adsorption energies are 0.30 and 0.57 eV for adsorption of CO and NO on NiO(100), respectively, and 0.14 and 0.22 eV for adsorption on MgO(100). We suggest that the stronger bonding to NiO(100) as compared to MgO(100) is due to the influence of the 3d electrons of NiO.

1. Introduction

In recent years many groups [1 to 8] have studied the properties of well-ordered oxide surfaces. Even though some qualitative understanding has been gained we are still far from a quantitative description even for the so-called simple systems. An example is the interaction of NO and CO with MgO(100) and NiO(100). Despite considerable effort it was not yet possible to establish agreement between theory and experiment (see Table 1).

Molecules bind to oxides via a bonding mechanism considerably different from metal surfaces. A CO molecule, for example, binds to metals via chemical bonds of varying strength involving charge exchanges [23]. Fig. 1 illustrates the bonding of CO to a Ni-metal atom via the so-called σ-donation/π-backdonation mechanism on the basis of a one-electron orbital diagram.

The σ- and π-interactions lead to a relative shift of those σ- and π-orbitals involved in the bond with respect to those orbitals not involved. The diagram reflects this via the correlation lines. This may be contrasted by the electrostatically dominated interaction between a CO molecule and a Ni ion in nickel oxide [11, 24]. There is a noticeable σ-repulsion between the CO carbon lone pair and the oxide leading to a similar shift of the CO 5σ-orbitals as in the case of the metal atom. However, there is no or little π-backdonation so that the CO π-orbitals are not modified [6, 7]. Conceptually, the situation is transparent and one would expect that a detailed calculation reveals the differ-

[1]) Corresponding author: phone: +49 30 8413 4222; Fax: +49 30 8413 4307; e-mail: Kuhlenbeck@FHI-Berlin.MPG.DE

Table 1
Table of literature data for adsorption of CO and NO on NiO(100) and Mg(100). BSSE: Basis Set Superposition Error, TDS: Thermal Desorption Spectroscopy, DFT: Density Functional Theory, IRS: InfraRed Spectroscopy, Clausius-Clapeyron: evaluation of pressure and temperature dependent IR intensities with the Clausius-Clapeyron equation, Redhead: evaluation of TDS data with the Redhead equation [22]

author	system	method	adsorption energy [eV]
Pacchioni and Bagus [9]	CO/NiO(100)	ab-initio cluster calculation	0.24
Klüner and Freund [10]	NO/NiO(100)	ab-initio cluster calculation, BSSE correction	≈ 0
Pöhlchen and Staemmler [11]	CO/NiO(100)	ab-initio cluster calculation, BSSE correction	0.03 to 0.1
Cappus et al. [12]	CO/NiO(100)/Ni(100)	TDS, Redhead	0.32
Vesecky et al. [13]	CO/NiO(100)/Ni(100)	IRS, Clausius-Clapeyron	0.45
Staemmler [14]	NO/NiO(100)	ab-initio cluster calculation, BSSE correction	0.1
Pöhlchen [15]	NO/NiO(100)	ab-initio cluster calculation, BSSE correction	<0.23
Kuhlenbeck et al. [16]	NO/NiO(100)/Ni(100) and NO/NiO(100)	TDS, Redhead	0.52
Nygren and Pettersson [17]	CO/MgO(100)	ab-initio cluster calculation, BSSE correction	0.08
Chen et al. [18]	CO/MgO(100)	DFT	0.28
Neyman et al. [19]	CO/MgO(100)	DFT, BSSE correction	0.11
He et al. [20]	CO/MgO(100)/Mo(100)	IRS, Clausius-Clapeyron TDS, Redhead	0.43 0.46
Furuyama et al. [21]	CO/MgO powder	IRS, Clausius-Clapeyron	0.15 to 0.17

ences quantitatively. However, as it turns out the description by ab-initio calculations is very much involved and today a full account cannot be given [17]. Theoretically, the prediction is that CO as well as NO bind very weakly to NiO [17]. The predicted binding energy of CO is of the order of 0.1 eV and is expected to be similar to CO binding to MgO(100), i.e. the influence of the Ni d-electrons should be negligible [17].

There seems to be a general trend that sophisticated theoretical calculations employing large basis sets yield bonding energies that are systematically smaller than the experimental determined ones. Therefore, it was argued that the experimental results might be due to adsorption on defects [17].

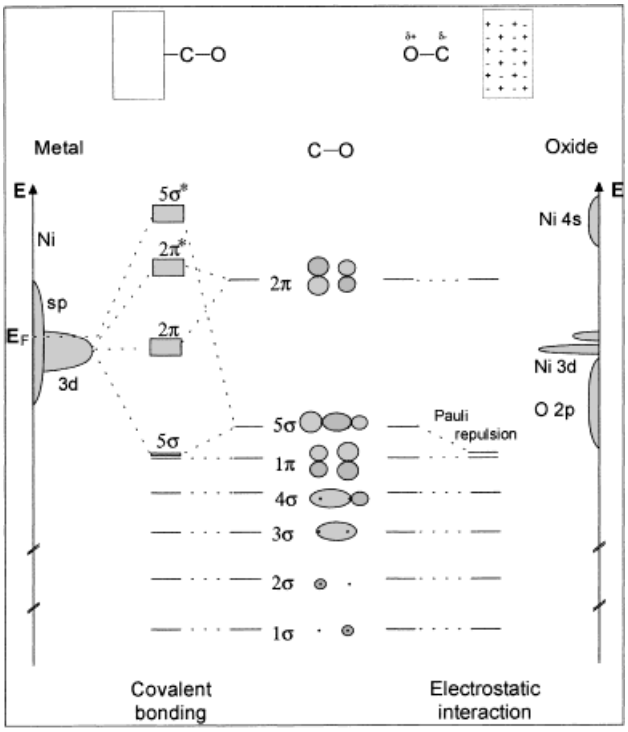

Fig. 1. Orbital diagram for the bonding of CO to Ni-metal (left) and to Ni-oxide (right)

In order to clarify the situation we have set up a TDS experiment which allows to scan the temperature linearly in the range between 25 and 400 K, using oxide single crystals cleaved in vacuum as samples. Substrates prepared by cleavage exhibit the smallest experimentally accessible defect density so that adsorption studies are not notably influenced by interaction of adsorbates with defects. Thus, adsorption experiments using such substrates provide data that are due to adsorption on regular sites. Therefore, they may be compared with theory.

2. Experimental

The substrates were single crystal oxide cylinders mounted on a helium cooled cold finger. Details of the set-up are depicted in Fig. 2. A tantalum filament wrapped around the lower part of the sample served for heating purposes and the temperature was determined with a NiCr–Ni thermocouple. Crystal cleavage was performed in situ with two blades guided by slits in the sample.

With our set-up the highest accessible heating rate was 2 K/s. Linearity of the temperature ramp was established via a PID regulator which allowed to keep the heating rate constant within 3%. Only at the beginning of the scan the deviation from the nominal heating rate could reach values of about 10%. In order to achieve a stable temperature signal, the thermocouple reference junction was kept at a constant temperature of (323 ± 0.02) K.

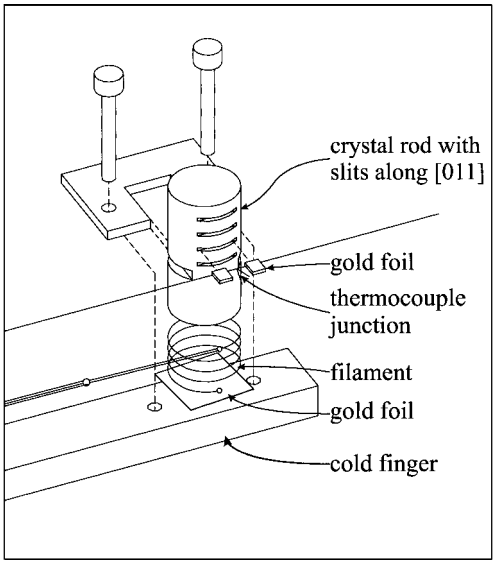

Fig. 2. Sample set-up used for the TDS experiments

The quality of the temperature signal was judged by monitoring the temperature of the multilayer desorption signal. For all TDS scans this was found to shift by not more than ± 2 K, centering around 30 K for CO. Deviations occurred mainly after mounting of a new sample so that they may be attributed to changed characteristics of the thermocouple. Within a set of data taken for a certain sample the multilayer desorption temperatures did not shift by more than ± 0.3 K. In order to be able to compare data from different sets of spectra these were shifted such that the CO multilayer desorption peaks were always at 30 K.

The mass spectrometer used for detection of the desorption signal was equipped with a so called Feulner cup [25] which was individually pumped. The inner walls were gold plated in order to minimize adsorption.

3. Results and Discussion

In Figs. 3 and 4 TDS data for CO and NO on vacuum-cleaved NiO(100) are compared with data for thin NiO(100) films grown by oxidation of Ni(100) [12, 16]. At temperatures of 30 and 56 K multilayer desorption for CO and NO, respectively, shows up. The pronounced features at higher temperatures correspond to desorption of the respective adsorbate at (sub)monolayer coverage. In the case of the CO adsorbate at 34 K desorption of the second layer is found and the states at 45 and 145 K for CO and NO, respectively, are due to adsorption on defects as concluded from data obtained from ion bombarded surfaces (not shown here). It is obvious that for both adsorbates the thin film data and the data of the cleaved samples agree well, demonstrating that in the case of NO and CO on NiO(100) the thin film data are comparable to those from the more perfect surfaces of the cleaved samples. The higher defect density of the thin film surfaces leads to small, but clearly visible additional peaks in the TDS data which show up as shoulders near to the main peak in the NO spectra. Nevertheless, the general shapes of the thin film spectra of both adsorbates are very similar to those of the cleaved samples.

For CO the shift of the peak maximum with increasing coverage indicates that at higher coverage repulsive lateral interactions come into play which may lead to occupation of energetically less favorable sites. This is not the case for the NO adsorbate which may be attributed to smaller lateral interactions and to the higher adsorption energy which makes adsorption more site specific and thus may inhibit compression of the layer involving site changes.

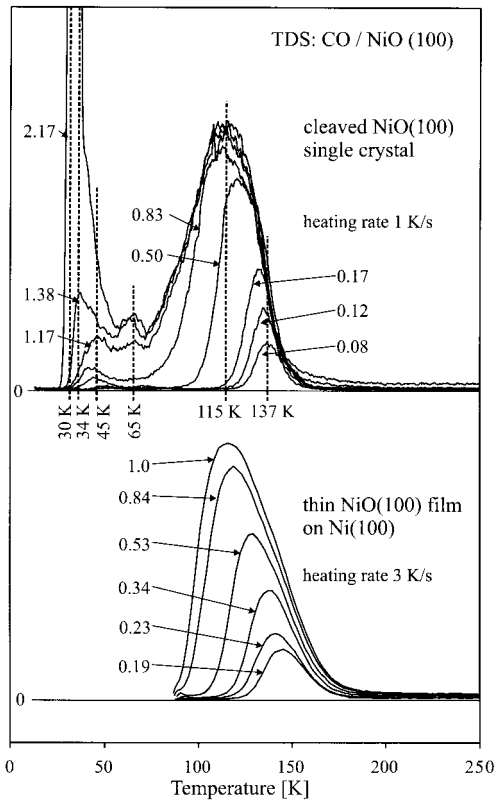

Fig. 3

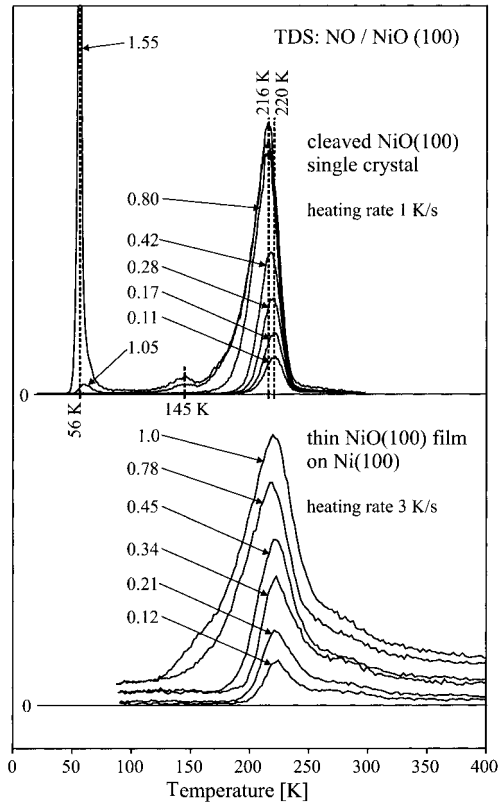

Fig. 4

Fig. 3. Thermal desorption spectra of CO on NiO(100) cleaved in vacuum (upper part) and CO on a thin NiO(100) film grown by oxidation of Ni(100) (lower part). The mass spectrometer was set to mass 28 (CO). CO doses are given relative to the dose needed to prepare a monolayer
Fig. 4. Thermal desorption spectra of NO on NiO(100) cleaved in vacuum (upper part) and NO on a thin NiO(100) film grown by oxidation of Ni(100) (lower part). The mass spectrometer was set to mass 30 (NO). NO doses are given relative to the dose needed to prepare a monolayer

TDS data for CO and NO on vacuum-cleaved MgO(100) are exhibited in Figs. 5 and 6. Multilayer desorption is found at 29 and 56 K for CO and NO, respectively. The small features around 45 and 100 K are likely due to defect adsorption since they saturate at rather low coverage. Desorption from layers with small coverage is found at 57 and 84 K for CO and NO, respectively.

The data for CO and NO on NiO(100) have been evaluated using the leading edge method and complete analysis. Details of the procedures may be found in [26 to 28]. Both methods determine the heat of adsorption as a function of the coverage of molecules already on the surface. The results of the evaluation are shown in Figs. 7 and 8. Both graphs exhibit a trend which is generally to be expected for laterally interacting adsorbate layers: the adsorption energy decreases with increasing coverage. At coverages near to unity the energies converge towards the multilayer values (0.09 and 0.18 eV for CO and NO, respectively [29]). At low coverage the lateral interactions are

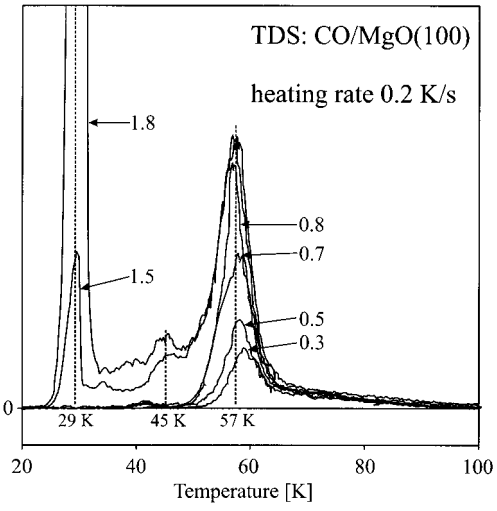

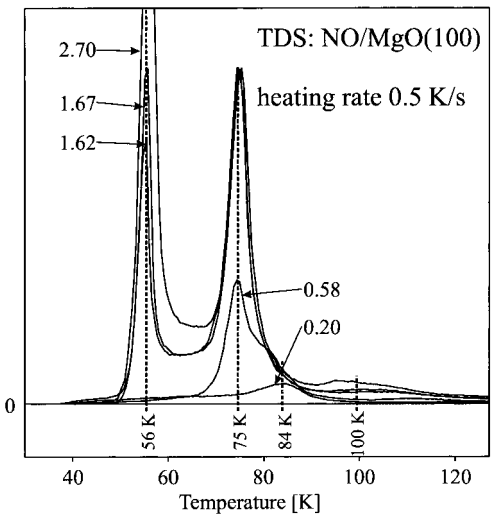

Fig. 5 Fig. 6

Fig. 5. Thermal desorption spectra of CO on MgO(100) cleaved in UHV. The mass spectrometer was set to mass 28 (CO). CO doses are given relative to the dose needed for the preparation of a monolayer

Fig. 6. Thermal desorption spectra of NO on MgO(100) cleaved in UHV. The mass spectrometer was set to mass 30 (NO). NO doses are given relative to the dose needed for the preparation of a monolayer

most likely small so that the corresponding adsorption energies may be compared with theoretical results since in the calculations lateral interactions have not been considered. As indicated in Figs. 7 and 8, the low coverage adsorption energies are 0.30 and 0.57 eV for CO and NO, respectively.

For NO and CO on MgO(100) the adsorption energies have been calculated via the Redhead equation [22] assuming a frequency factor of $10^{13}\ s^{-1}$. This gave values of 0.14 and 0.22 eV for CO and NO, respectively, in the low coverage regime. The result for CO corresponds well to LEED (Low Energy Electron Diffraction) results obtained by Audibert et al. [30] who observed ordered CO superstructures only at temperatures below 55 K. It also fits well to earlier data of CO on MgO powder where a binding energy of 0.15 to 0.17 eV was deduced [21], see Table 1. He et al. [20] obtained a binding energy of 0.43 eV for CO on a thin MgO(100) film on Mo(100). This result is at variance with our data indicating that in this case adsorption was strongly influenced by surface defects.

Table 2
Compilation of low-coverage bonding energies for NO and CO on NiO(100) and MgO(100) obtained in this work

	NiO(100)	MgO(100)
CO	0.30 eV	0.14 eV
NO	0.57 eV	0.22 eV

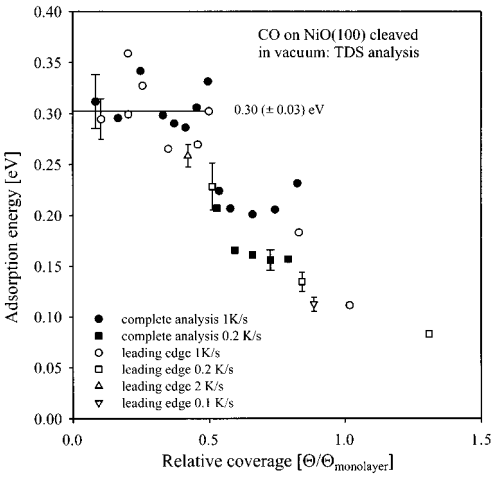

Fig. 7

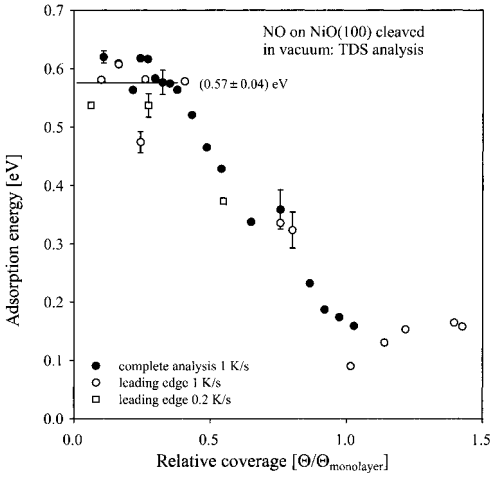

Fig. 8

Fig. 7. Adsorption energy of CO on NiO(100) cleaved in vacuum as a function of coverage. The data have been determined from TDS spectra like those shown in Fig. 3 (upper part) using the leading edge method [26] and complete analysis [27]. TDS data taken with heating rates of 0.1, 0.2, 1 and 2 K/s have been used

Fig. 8. Adsorption energy of NO on NiO(100) cleaved in vacuum as a function of coverage. The data have been determined from TDS spectra like those shown in Fig. 4 (upper part) using the leading edge method [26] and complete analysis [27]. TDS data taken with heating rates of 0.2 and 1 K/s have been used

The low coverage adsorption energies for CO and NO on NiO(100) and MgO(100) are compiled in Table 2. According to theory the interaction of the adsorbates with MgO(100) and NiO(100) should be similar since the bonding should be mainly electrostatic in nature [17] (the electric fields at the surfaces of NiO(100) and MgO(100) are similar). However, according to Table 2 the bonding energies are different with the higher values being obtained for NiO(100). Thus, it may be the case that covalent interactions involving the Ni3d electrons play a role in the adsorbate–substrate interaction which should not be the case according to theory.

As far as it concerns the BSSE corrected calculations listed in Table 1 which are expected to yield qualitatively better results as compared to the non-corrected calculations, it appears that the theoretical results for adsorption on MgO(100) are in general in line with our results whereas a similar favorable comparison cannot be made for NiO(100). Thus, it may be needed to re-investigate the role of the Ni3d electrons in future theoretical studies.

4. Summary

Using TDS we have determined the adsorption energies of CO and NO on NiO(100) and MgO(100). Adsorption energies of (0.30 ± 0.03) eV for CO/NiO(100), (0.57 ± 0.04) eV for NO/NiO(100), 0.14 eV for CO/MgO(100) and 0.22 eV for NO/MgO(100) were obtained for the low coverage regime. The results for vacuum-cleaved NiO(100) are in line with adsorption energies obtained for thin NiO(100) films on NiO(100) whereas for

CO/MgO(100) our results do not agree with values for MgO(100) films on Mo(100). The TDS results for CO on MgO(100) agree reasonably well with recent ab initio calculations but they are at variance for NO and CO on NiO(100) which we tentatively attribute to covalent interactions of the adsorbates with Ni3d electrons.

Acknowledgement We acknowledge Dr. Thorsten Klüner and Prof. L. G. M. Pettersson for valuable and fruitful discussions.

References

[1] V. E. HENRICH and P. A. COX, The Surface Science of Metal Oxides, Cambridge University Press, Cambridge 1994.
[2] H.-J. FREUND, H. KUHLENBECK, and V. STAEMMLER, Rep. Progr. Phys. **59**, 283 (1996).
[3] G. RENAUD, Surf. Sci. Rep. **32**, 1 (1998).
[4] C. T. CAMPBELL, Surf. Sci. Rep. **27**, 1 (1997).
[5] C. XU and D. W. GOODMAN, in: Handbook of Heterogeneous Catalysis, Eds. G. ERTL, H. KNÖZINGER, and J. WEITKAMP, Chap. 4.6, VCH, Weinheim 1997.
[6] H.-J. FREUND, Angewandte Chemie – Internat. Ed. **36**, 452 (1997).
[7] M. BÄUMER, J. LIBUDA, and H.-J. FREUND, Metal Deposits on Thin Well Ordered Oxide Films: Morphology, Adsorption and Reactivity, in: Nato Adv. Study Inst., NATO ASI Series, Ser. E, Eds. R. M. LAMBERT and G. PACCHIONI, Vol. 331, Kluwer Academic Press, Dordrecht 1997 (p. 61).
[8] C. HENRY, Surf. Sci. Rep. **31**, 231 (1998).
[9] G. PACCHIONI and P. S. BAGUS, in: Adsorption on Ordered Surfaces of Ionic Solids and Thin Films, Eds. H.-J. FREUND and E. UMBACH, Vol. 33, Springer Series Surf. Sci., Springer-Verlag, Berlin 1993 (p. 180).
[10] T. KLÜNER and H.-J. FREUND, private communication.
[11] M. PÖHLCHEN and V. STAEMMLER, J. Chem. Phys. **97**, 2583 (1992).
[12] D. CAPPUS, J. KLINKMANN, H. KUHLENBECK, and H.-J. FREUND, Surf. Sci. **325**, L421 (1995).
[13] S. M. VESECKY, X. XU, and D. W. GOODMAN, J. Vac. Sci. Technol. A **12**, 2114 (1994).
[14] V. STAEMMLER, see [9] (p. 169).
[15] M. PÖHLCHEN, PhD Thesis, Ruhr-Universität Bochum (Germany), 1992.
[16] H. KUHLENBECK, G. ODÖRFER, R. JAEGER, G. ILLING, M. MENGES, TH. MULL, H.-J. FREUND, M. PÖHLCHEN, V. STAEMMLER, S. WITZEL, C. SCHARFSCHWERDT, K. WENNEMANN, T. LIEDTKE, and M. NEUMANN, Phys. Rev. B **43**, 1969 (1991).
[17] M. A. NYGREN and L. G. M. PETTERSSON, J. Chem. Phys. **105**, 9339 (1996).
[18] L. CHEN, R. WU, and N. KIOUSSIS AN Q. ZHANG, Chem. Phys. Lett. **290**, 255 (1998).
[19] K. M. NEYMAN, S. PH. RUZANKIN, and N. ROESCH, Chem. Phys. Lett. **246**, 546 (1995).
[20] J.-W. HE, C. A. ESTRADA, J. S. CORNEILLE, M.-C. WU, and D. W. GOODMAN, Surf. Sci. **261**, 164 (1992).
[21] S. FURUYAMA, H. FUJII, M. KAWAMURA, and T. MORIMOTO, J. Phys. Chem. **82**, 1028 (1978).
[22] P. A. REDHEAD, Vacuum **12**, 203 (1962).
[23] M. HENZLER and W. GÖPEL, Oberflächenphysik des Festkörpers, Teubner-Verlag, Stuttgart 1991.
[24] K. M. NEYMAN, G. PACCHIONI, and N. RÖSCH, in: Recent Developments and Applications of Modern Density Functional Theory and Computational Chemistry, Vol. 4, Elsevier, 1996 (p. 569).
[25] P. FEULNER and D. MENZEL, J. Vac. Sci. Technol. A **17**, 662 (1980).
[26] E. HABENSCHADEN and J. KÜPPERS, Surf. Sci. **138**, L147 (1984).
[27] H. PFNÜR, P. FEULNER, and D. MENZEL, J. Chem. Phys. **79**, 4613 (1983).
[28] C. N. CHITTENDEN, E. D. PYLANT, A. L. SCHWANER, and J. M. WHITE, Thermal Desorption and Mass Spectrometry, in: The Handbook of Surface Imaging and Visualization, Ed. A. T. HUBBARD, CRC Press, Boca Raton 1995.
[29] H. SCHLICHTING and D. MENZEL, Rev. Sci. Instrum. **64**, 2013 (1993).
[30] P. AUDIBERT, M. SIDOUMOU, and J. SUZANNE, Surf. Sci. **273**, 467 (1992).